Experimental signatures of an absorbing-state phase transition in an open driven many-body quantum system

Ricardo Gutiérrez,[1,2] Cristiano Simonelli,[3,4] Matteo Archimi,[4] Francesco Castellucci,[4] Ennio Arimondo,[3,4,5] Donatella Ciampini,[3,4,5] Matteo Marcuzzi,[1,2] Igor Lesanovsky,[1,2] and Oliver Morsch[3,4]

[1] *School of Physics and Astronomy, University of Nottingham, Nottingham, NG7 2RD, UK*
[2] *Centre for the Mathematics and Theoretical Physics of Quantum Non-Equilibrium Systems, University of Nottingham, Nottingham, NG7 2RD, UK*
[3] *INO-CNR, Via G. Moruzzi 1, 56124 Pisa, Italy*
[4] *Dipartimento di Fisica "E. Fermi", Università di Pisa, Largo Bruno Pontecorvo 3, 56127 Pisa, Italy*
[5] *CNISM UdR Dipartimento di Fisica "E. Fermi", Università di Pisa, Largo Bruno Pontecorvo 3, 56127 Pisa, Italy*

(Dated: September 19, 2017)

Understanding and probing phase transitions in non-equilibrium systems is an ongoing challenge in physics. A particular instance are phase transitions that occur between a non-fluctuating absorbing phase, e.g., an extinct population, and one in which the relevant order parameter, such as the population density, assumes a finite value. Here we report the observation of signatures of such a non-equilibrium phase transition in an open driven quantum system. In our experiment rubidium atoms in a quasi one-dimensional cold disordered gas are laser-excited to Rydberg states under so-called facilitation conditions. This conditional excitation process competes with spontaneous decay and leads to a crossover between a stationary state with no excitations and one with a finite number of excitations. We relate the underlying physics to that of an absorbing state phase transition in the presence of a field (i.e. off-resonant excitation processes) which slightly offsets the system from criticality. We observe a characteristic power-law scaling of the Rydberg excitation density as well as increased fluctuations close to the transition point. Furthermore, we argue that the observed transition relies on the presence of atomic motion which introduces annealed disorder into the system and enables the formation of long-ranged correlations. Our study paves the road for future investigations into the largely unexplored physics of non-equilibrium phase transitions in open many-body quantum systems.

PACS numbers: 32.80.Ee, 64.70.qj

Absorbing state phase transitions are among the simplest non-equilibrium phenomena displaying critical behavior and universality. They can occur for instance in models describing the growth of bacterial colonies or the spreading of an infectious disease among a population (see, e.g., [1–3]). Once an absorbing state, e.g., a state in which all the bacteria are dead, is reached, the system cannot escape from it [4]. However, there might be a regime where the proliferation of bacteria overcomes the rate of death and thus a finite stationary population density is maintained for long times. The transition between the absorbing and the active state may be continuous, with observables displaying universal scaling behaviour [5–9]. Although conceptually of great interest, the unambiguous observation of even the simplest non-equilibrium universality class – directed percolation – is challenging and has only been achieved in recent years in a range of soft-matter systems and fluid flows [10–16] (see also the references in [11, 12]). The exploration of such universal non-equilibrium phenomena is currently an active topic across different disciplines with a number of open questions concerning, among others, their classification, the role of disorder, and quantum effects. In particular, cold atomic systems have proven to constitute a versatile platform for probing this and related physics [17–26].

Here we experimentally observe signatures of an absorbing state phase transition in a driven open quantum system formed by a gas of cold atoms. We laser-excite high-lying Rydberg states under so-called *facilitation conditions* [27–30], whereby an excited atom favours the excitation of a nearby atom at a well-defined distance. This process can lead to an avalanche-like spreading of excitations [19, 20, 22, 23] and competes with spontaneous radiative decay, which drives the system towards a state without Rydberg excitations. As a result, the system displays a crossover between an absorbing state and a stationary state with a finite Rydberg excitation density. We identify signatures suggesting that this crossover is in fact a smoothed out continuous phase transition. An intriguing feature of this phase transition is that it appears to require atomic motion in order to occur in the disordered atomic gas considered here.

In our experiments we prepare cold atomic samples of ^{87}Rb atoms in a magneto-optical trap (MOT) at an approximate temperature of 150 μK. The density distribution is Gaussian with width $\sigma = 230$ μm and peak density $n_0 = 4.5 \times 10^{10}\,\mathrm{cm}^{-3}$. The external driving, consisting of two co-propagating laser beams of wavelengths 420 and 1013 nm, couples the ground state $|g\rangle$ and the high-lying (Rydberg) state 70S $|r\rangle$. Atoms i and j in

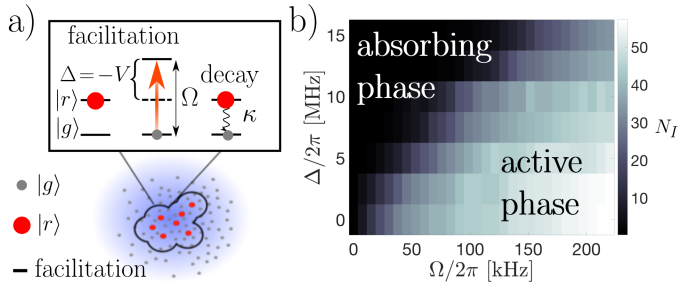

FIG. 1. **Schematic diagram of the experimental setting and processes involved, and experimental phase diagram.** (a) Atomic cloud with ground state atoms (gray discs), excited atoms (red discs) and atoms in the propagating facilitation region (black curved line). In the upper panel, the processes driving the dynamics are highlighted: facilitated excitations, for which the detuning Δ compensates the interaction V, are shown on the left (Ω is the Rabi frequency), and atomic decay on the right (κ is the decay rate). (b) Phase diagram showing the number of excitations N_I in the stationary state as a function of Ω and Δ. We observe a crossover from an absorbing state with essentially zero excitations to a fluctuating phase with a finite number of excitations.

state $|r\rangle$ at positions $\mathbf{r}_i$ and $\mathbf{r}_j$ interact [31–36] through van der Waals interactions $V_{ij} = C_6/|\mathbf{r}_i - \mathbf{r}_j|^6$ with a positive dispersion coefficient $C_6 = h \times 869.7$ GHz μm^6 [37]. The coupling strength between $|g\rangle$ and $|r\rangle$ is given by the (two-photon) Rabi frequency Ω, and the excitation lasers can be detuned by an amount Δ from resonance. The dephasing rate (due to the laser linewidth and residual Doppler broadening) is $\gamma = 4.4$ MHz, which is greater than the maximum value of $\Omega = 2\pi \times 250$ kHz. The system is thus in the (incoherent) strongly dissipative regime [29, 38–41]. We focus on blue detuning $\Delta > 0$, for which previous theoretical and experimental work [19, 20, 22, 23, 30] has shown that, in the presence of strong dephasing, the aforementioned facilitation mechanism increases the probability to excite (or de-excite) atoms in a spherical shell of radius $r_{\rm fac} = (C_6/\hbar\Delta)^{1/6}$ around an excited atom [29, 30]. The laser beam at 420 nm is focused to a waist of around 8 μm, which is comparable to $r_{\rm fac}$ in this parameter regime, effectively reducing the excitation dynamics to one dimension (1D).

Figure 1 (a) schematically shows the main processes occurring in our system: a configuration of ground state atoms (gray discs) and Rydberg excitations (red discs) is shown (displayed here in a 2D setting for ease of visualization), and the collective facilitation shell that results from the presence of a cluster of excitations is highlighted (black continuous line). The dynamics is characterized by the competition between facilitation and the spontaneous decay of excitations at a rate $\kappa = 12.5$ kHz [42]. The system eventually reaches a stationary state that depends on the relative strength of these two processes.

Experimentally, we study the resulting stationary state by applying the following protocol. At the beginning of an experimental cycle (during which the MOT beams are switched off), we excite $6 \pm \sqrt{6}$ seed atoms (according to a Poissonian seed distribution) in 0.3 μs with the excitation laser on resonance with the Rydberg transition. Thereafter, the atoms are excited at finite (two-photon) detuning $\Delta > 0$ and Rabi frequency Ω for a duration of 1.5 ms, which is much longer than the lifetime $1/\kappa$ of the 70S state [42]. Immediately after that, an elecric field is applied that field ionizes all the Rydberg atoms with principal quantum number $n \gtrsim 40$ and accelerates the ions towards a channeltron, where they are counted with a detection efficiency of 40%. The observables of interest are based on the distribution of the number of detected ions at the end of each run. The procedure is repeated 100 times for each set of parameters, with a repetition rate of 4 Hz, in order to get reliable estimates of the mean N_I and the variance $\Delta {N_I}^2$ of the number of detected ions.

In Fig. 1 (b) we display the phase diagram resulting from this measurement procedure. The order parameter N_I is plotted as a function of Ω and Δ. One can clearly see a crossover between an absorbing state, with essentially zero excitations for sufficiently small Ω, and a phase with a finite number of excitations for larger Ω. In the remainder of this work we will focus on the nature of this crossover.

To provide some qualitative theoretical insight, we first conduct a simple mean-field analysis based on a 1D system that follows the same dynamical rules. Adopting the semi-classical description of Ref. [30], the (de-)excitation of atom i occurs at a rate Γ_i that depends on the configuration of neighbouring excitations. If we neglect the correlations between atoms, the average $\langle n_i \rangle$ of the number operator $n_i \equiv |r\rangle_i\langle r|$ acting on site i evolves in time according to

$$\partial_t \langle n_i(t)\rangle = \langle -|\Gamma_i(1-2n_i)|P(t)\rangle - \kappa\langle n_i(t)\rangle, \qquad (1)$$

where $|P(t)\rangle \equiv \sum_{\mathcal{C}} P(\mathcal{C};t)|\mathcal{C}\rangle$, the kets $|\mathcal{C}\rangle$ are the classical atomic configurations in the number basis (the eigenbasis of all the n_i), $P(\mathcal{C};t)$ is the probability of configuration $|\mathcal{C}\rangle$ at time t, and $|-\rangle \equiv \sum_{\mathcal{C}} |\mathcal{C}\rangle$. At this point we introduce the simplifying assumption that the rate Γ_i can take only two values: the facilitated rate $\Gamma_{\rm fac}$ if the i-th atom lies in the facilitation shell of an existing excitation, or otherwise the spontaneous rate $\Gamma_{\rm spon}$, corresponding to the rate in the absence of nearby excitations,

$$\Gamma_{\rm fac} \equiv \Omega^2/2\gamma;\ \Gamma_{\rm spon} \equiv \left(\Omega^2/2\gamma\right)\left[1+\Delta^2/\gamma^2\right]^{-1}. \qquad (2)$$

In a coarse-grained description of the system, where $n \equiv N_{\mathcal{V}}^{-1}\sum_{i\in\mathcal{V}} n_i$ is the fraction of excited atoms in a region of space $\mathcal{V}$ (spanning a few facilitation radii) with $N_{\mathcal{V}}$ atoms in it, we expect the average rate to be $n\,\Gamma_{\rm fac} + (1-n)\,\Gamma_{\rm spon}$. Assuming homogeneity, the spatially averaged dynamics is given by

$$\dot{n} = \Gamma_{\rm fac} n(1-2n) + \Gamma_{\rm spon}(1-n)(1-2n) - \kappa n. \qquad (3)$$

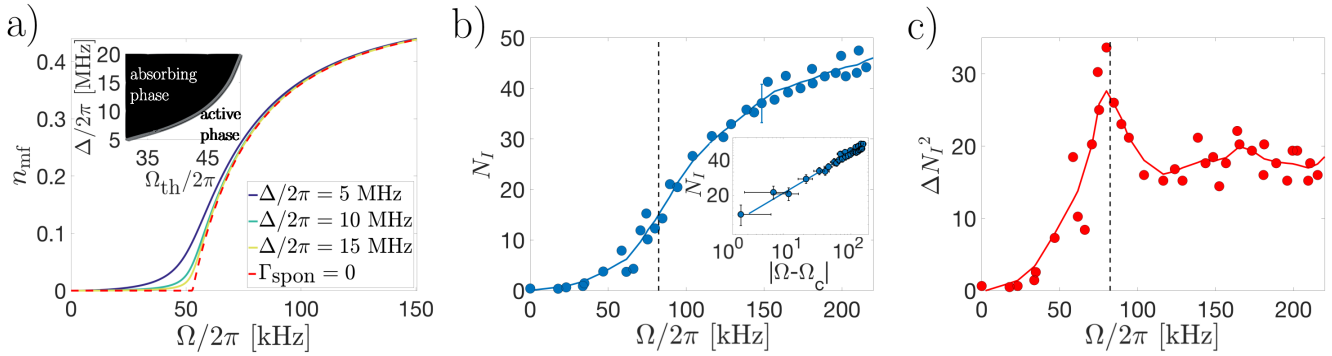

FIG. 2. **Mean field stationary density, and experimental mean and variance of the number of excitations.** (a) Density of excitations $n_{\rm mf}$ in the stationary state of the two-level mean-field model (see text) as a function of the Rabi frequency Ω for different values of the detuning Δ. The correspondence between the detuning and the ratio between facilitated and spontaneous rates is as follows: for $\Delta/2\pi = 5$ MHz the ratio is $\Gamma_{\rm spon}/\Gamma_{\rm fac} = 19.2 \cdot 10^{-3}$, for $\Delta/2\pi = 10$ MHz it is $\Gamma_{\rm spon}/\Gamma_{\rm fac} = 4.9 \cdot 10^{-3}$ and for $\Delta/2\pi = 15$ MHz it is $\Gamma_{\rm spon}/\Gamma_{\rm fac} = 2.2 \cdot 10^{-3}$. The red dashed line shows the behavior in the absence of spontaneous (de-)excitations for $\Delta/2\pi = 15$ MHz, which shows a continuous phase transition. The inset shows the value of Ω at which the density reaches 0.01 – which we denote $\Omega_{\rm th}$ – as a function of Δ. (b) Average number of excitations at the end of the 1.5 ms time window in the experiment for $\Delta/2\pi = 10$ MHz. One representative error bar is shown, corresponding to one standard deviation. *Inset*: same data in loglog plot for $\Omega > \Omega_c = 2\pi \times (82.4 \pm 0.2)$ kHz. A power law nonlinear fit based on the expression $\log(N_I) = \alpha + \beta \log(\Omega - \Omega_c)$ has been applied to the data, yielding an exponent $\beta = 0.31 \pm 0.04$. The horizontal error bars correspond to a relative uncertainty of $\pm 5\%$ in the measurement of Ω due to fluctuations in the laser intensity, and possible misalignments of the beams. The vertical error bars correspond to the measured standard deviations of the number of excitations. (c) Variance of the number of excitations as a function of $\Omega/2\pi$ based on the same experimental data. The continuous line in panels (b) and (c) is a guide to the eye and results from a sliding average, and the dashed vertical lines indicate the position of the critical point.

We first consider the limit $\Gamma_{\rm spon}/\Gamma_{\rm fac} \to 0$ (i.e. $\Delta/\gamma \to \infty$), where the dynamics is purely governed by the competition between facilitation and decay. The stationary state solution for $\Gamma_{\rm fac} < \kappa$ is the state without excitations, which constitutes an absorbing state of the dynamics. For $\Gamma_{\rm fac} \geq \kappa$ facilitation prevails over decay, and the absorbing state becomes unstable, leading to a finite density stationary state,

$$n_{\rm mf} = \begin{cases} 0, & \text{if } \Gamma_{\rm fac} < \kappa, \\ (1 - \kappa/\Gamma_{\rm fac})/2, & \text{otherwise.} \end{cases} \tag{4}$$

As $n_{\rm mf}$ is continuous at $\Gamma_{\rm fac} = \kappa$, but its first derivative with respect to $\Gamma_{\rm fac}$ is not, this indicates the existence (at the mean-field level) of a non-equilibrium continuous phase transition between an absorbing state with zero excitations and a fluctuating phase with a finite density [6]. Since in our experiment atoms in the 70S state can migrate (via black-body radiation) to other Rydberg states, we additionally devised a three-level model taking into account this effect, which shows the same qualitative behavior (see [42]).

In Fig. 2 (a) we plot $n_{\rm mf}$ as a function of the Rabi frequency Ω for different values of the detuning Δ, using the experimental values of the dephasing and decay rates. For the largest value of Δ, we also explore the stationary state in the absence of spontaneous excitations, $\Gamma_{\rm spon} = 0$ (see the red dashed line), which shows the aforementioned phase transition. For non-vanishing $\Gamma_{\rm spon}/\Gamma_{\rm fac}$, $n_{\rm mf}$ is always positive and the non-analyticity at $\Gamma_{\rm fac} = \kappa$ is smoothed out into a crossover (see the continuous lines). For larger values of Δ, as $\Gamma_{\rm spon}$ is suppressed, the system is expected to be closer to the critical point. In the inset, we show the position of the threshold $\Omega_{\rm th}$, which we set to be the value of the Rabi frequency for which $n_{\rm mf} = 0.01$. We take this to be an approximate measure of the onset of the crossover between the absorbing phase and the active phase away from the critical point. We conjecture that the same physics lies at the basis of the phase diagram in Fig. 1, which would thus signal the presence of a smoothed phase transition in the experiment. The smoothness stems from the spontaneous rate $\Gamma_{\rm spon}$ which acts like a field that off-sets the system away from criticality. By substituting our estimates of the experimental parameters, we find $\Gamma_{\rm spon}/\Gamma_{\rm fac}$ to be of the order of 10^{-3} for $\Omega/2\pi = 125$ kHz and $|\Delta/2\pi| = 10$ MHz [42].

In the presence of a continuous phase transition, we would expect the experimental data to show a smoothed-out singularity in the fluctuations and a power-law behavior in the number of excitations [6]. This is, indeed, compatible with what we observe. In Fig. 2 (b) the number of excitations N_I is plotted as a function of Ω for a fixed detuning $\Delta = 2\pi \times 10$ MHz. The continuous line results from a sliding average, and is meant as a guide to the eye. In Fig. 2 (c) we show the variance of the number of excitations $\Delta N_I{}^2$ for the same data as in (b), which displays a clear peak around $\Omega/2\pi = 80$ kHz. Ap-

proaching a critical point, the correlation length diverges, and global density fluctuations should correspondingly diverge. In the inset of Fig. 2 (b), N_I is plotted on a reduced interval in logarithmic scale. Since the position of the peak gives the approximate location of the critical Rabi frequency, Ω_c is chosen in its neighborhood as the value that maximizes the goodness of the nonlinear fit. This procedure yields a value of $\Omega_c = 2\pi \times (82.4 \pm 0.2)$ kHz [dashed vertical line in Fig. 2 (b) and (c)] and a power-law dependence $N_I \sim (\Omega - \Omega_c)^\beta$ with an exponent $\beta \approx 0.31 \pm 0.04$ (see below a discussion of the significance of this result).

We turn now to a closer inspection of the role of disorder in the atomic cloud. This will highlight the relevance of atomic motion as a central ingredient for the observed physics [26]. In order to undergo a phase transition, the system must establish correlations over mesoscopic length scales, and to analyze whether this is possible we have to consider two experimental features that so far have not been discussed: positional disorder and atomic motion. To this end, we use an effective 1D lattice model comprising L sites occupied by N atoms ($L > N$) located at random positions. We first address the hypothetical situation in which the positions are frozen for the duration of the experiment, so that the spatial configuration induces *quenched* disorder on the excitation rates. A prerequisite for the formation of a large cluster of excitations is the existence of a large number of atoms located at a distance $r_{\rm fac}$ from each other, and a simple argument shows that the probability of finding such clusters is exponentially suppressed in the cluster size [42]. For example, if we estimate the effective length of the cloud to be the distance between the positions at which the density drops to 1% of the value at the peak (on either side), which gives $L_{\rm eff} \simeq 990$ μm, and if we consider there are $k = 10$ sites per $r_{\rm fac}$, the experimental conditions translate into a density $\rho \equiv N/L \approx 0.3$. Under these conditions, the resulting probability of occurrence of an occupied sublattice of size $L_{\rm eff}/10 \approx 15\, r_{\rm fac}$ is considerably smaller than 10^{-6}. This illustrates the fact that correlations over mesoscopic length scales are extremely unlikely to develop in the cloud.

However, in our experiment the timescales are too long for this frozen gas picture to hold. In fact, the mean atomic velocity of our samples translates into a mean displacement of around 0.19 m/s (for $T = 150$ μK), meaning that on the timescale of an experimental cycle an atom can traverse a distance comparable to the width of the cloud. The excitation dynamics proceeds on an ever changing background, which corresponds to *annealed* disorder. To study this effect we use the lattice model discussed above, with the atomic motion parametrized by the mobility λ, which is the rate at which atoms jump to neighboring sites (so long as they do not violate the single occupancy condition). The inclusion of these jump processes is a minimal way to account for thermal motion

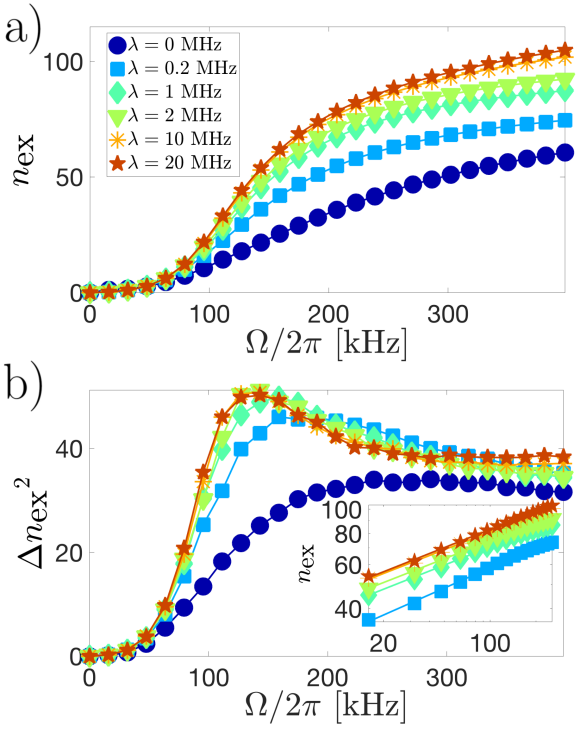

FIG. 3. **Mean and variance of the number of excitations as a function of $\Omega/2\pi$ in a 1D model with atomic motion.** Results based on a chain of $L = 1500$ sites and $N = 450$ atoms with the experimental laser and atomic level parameters, and a range of mobility λ based on the experimental atomic motion. (a) Mean number of excitations $n_{\rm ex}$ as a function of $\Omega/2\pi$ for mobilities $\lambda = 0$ (quenched disorder), 0.2, 1, 2, 10, 20 MHz. (b) Fluctuations of the excitation number $\Delta {n_{\rm ex}}^2$ as a function of $\Omega/2\pi$ for different λ [color code and markers as in panel (a)]. The inset shows a logarithmic plot of $n_{\rm ex}$ vs $(\Omega - \Omega_c)/2\pi$, where Ω_c is defined to be the value of Ω where the fluctations reach a peak, and associated power law fits.

as well as mechanical effects due to repulsion between Rydberg states. For the spreading of excitations to become possible, it is to be expected that atomic motion should be such that excitations have at least an atom going through their facilitation shell before decaying.

In Fig. 3 (a) and (b) we plot the mean number of excitations $n_{\rm ex}$ and the variance $\Delta {n_{\rm ex}}^2$, respectively, as a function of Ω for a chain with $k = 10$ sites per facilitation distance $r_{\rm fac}$ and $L = kL_{\rm eff}/r_{\rm fac} = 1500$. The density of occupied sites of choice, $\rho = 0.3$ ($N = 450$), and the range of λ values considered [see panel (a) for the color coding] have been adjusted to match the experimental conditions (see [42]), while the rest of the parameters are those of the experiment (with $\Delta = 2\pi \times 10\,$MHz). For $\lambda = 0$ (quenched disorder) the growth of $n_{\rm ex}$ with Ω is mild and the fluctuations $\Delta {n_{\rm ex}}^2$ do not display a peak. As λ is increased (i.e., for time-dependent disorder), however, the growth becomes more abrupt and the fluctuations display a clear peak. In the inset of Fig. 3 (b) we include

a logarithmic plot of $n_{\rm ex}$ against $(\Omega-\Omega_c)$ for $\lambda > 0$, where Ω_c is the position of the peak. The results are compatible with a power law dependence $n_{\rm ex} \sim (\Omega-\Omega_c)^\beta$, especially for large mobilities, with an exponent that appears to saturate around $\beta \approx 0.25 \pm 0.04$. From this we conclude that in our model, and probably in our experimental system, atomic motion proves crucial for the emergence of pronounced fluctuations and scaling behavior.

In summary, we have presented experimental data that show a crossover between an absorbing phase without Rydberg excitations and an active phase with a finite fraction of Rydberg excitations in an open dissipative atomic gas. Evidence for the existence of a underlying non-equilibrium continuous phase transition has been provided. In fact, the effective mean-field model as well as the extracted scaling exponent suggest a connection to directed percolation (DP), which is one of the simplest non-equilibrium universality classes. DP has previously been predicted to emerge in Rydberg lattice systems [43]. The scaling exponent extracted from the experimental data is compatible with that of DP in one dimension, $\beta_{\rm DP} = 0.276486(8)$ [6]. A crucial issue of the current experiment is the nature and role of disorder. The point we have emphasized above, namely that quenched disorder heavily distorts the critical behavior, whereas annealed disorder does not, has been established for DP via field-theoretical and numerical approaches [6, 44–46]. A future goal is to fully characterize and classify the non-equilibrium phases of driven Rydberg gases, e.g., through more precise measurements of static and dynamic exponents and also a field-theoretical study of the universal properties. An exciting perspective is that Rydberg gases allow the controlled inclusion of quantum effects, e.g., by reducing the dephasing rate. Future studies will thus potentially access new dynamical regimes that go beyond the current body of knowledge on out-of-equilibrium phase transitions, which is largely focused on classical many-body systems [6, 7].

Acknowledgements — RG, MM and IL would like to thank Juan P. Garrahan and Carlos Pérez-Espigares for useful discussions. The research leading to these results has received funding from the European Research Council under the European Union's Seventh Framework Programme (FP/2007-2013) / ERC Grant Agreement No. 335266 (ESCQUMA), the EU-FET grant HAIRS 612862 and from the University of Nottingham. Further funding was received through the H2020-FETPROACT-2014 grant No. 640378 (RYSQ). RG acknowledges the funding received from the European Union's Horizon 2020 research and innovation programme under the Marie Sklodowska-Curie grant agreement No. 703683. We also acknowledge financial support from EPSRC Grant no. EP/M014266/1. Our work has benefited from the computational resources and assistance provided by the University of Nottingham High Performance Computing service.

[1] P. Grassberger. On the critical behavior of the general epidemic process and dynamical percolation. *Math. Biosci.*, 63(2):157 – 172, 1983.

[2] J.-T. Kuhr, M. Leisner, and E. Frey. Range expansion with mutation and selection: dynamical phase transition in a two-species Eden model. *New J. Phys.*, 13(11):113013, 2011.

[3] J. A. Bonachela, M. A. Muñoz, and S. A. Levin. Patchiness and demographic noise in three ecological examples. *J. Stat. Phys.*, 148(4):724–740, 2012.

[4] N. Richter-Dyn and N. S. Goel. On the extinction of a colonizing species. *Theor. Popul. Biol.*, 3(4):406 – 433, 1972.

[5] P. Grassberger. Directed percolation: results and open problemsk. In S. Puri et al., editor, *Nonlinearities in complex systems, proceedings of the 1995 Shimla conference on complex systems*. Narosa Publishing, New Dehli, 1997.

[6] H. Hinrichsen. Non-equilibrium critical phenomena and phase transitions into absorbing states. *Adv. Phys.*, 49(7):815–958, 2000.

[7] G. Ódor. Universality classes in nonequilibrium lattice systems. *Rev. Mod. Phys.*, 76:663–724, 2004.

[8] S. Lübeck. Universal scaling behavior of non-equilibrium phase transitions. *Int. J. Mod. Phys. B*, 18(31n32):3977–4118, 2004.

[9] J. Marro and R. Dickman. *Nonequilibrium phase transitions in lattice models*. Cambridge University Press, Cambridge, 2005.

[10] P. Rupp, R. Richter, and I. Rehberg. Critical exponents of directed percolation measured in spatiotemporal intermittency. *Phys. Rev. E*, 67(3):036209, 2003.

[11] K. A. Takeuchi, M. Kuroda, H. Chaté, and M. Sano. Directed percolation criticality in turbulent liquid crystals. *Phys. Rev. Lett.*, 99:234503, 2007.

[12] K. A. Takeuchi, M. Kuroda, H. Chaté, and M. Sano. Experimental realization of directed percolation criticality in turbulent liquid crystals. *Phys. Rev. E*, 80:051116, 2009.

[13] G. Lemoult, Liang Shi, Kerstin Avila, Shreyas V. Jalikop, Marc Avila, and Bjorn Hof. Directed percolation phase transition to sustained turbulence in Couette flow. *Nat. Phys.*, 12(3):254–258, 2016.

[14] M. Sano and K. Tamai. A universal transition to turbulence in channel flow. *Nat. Phys.*, 12(3):249–253, 2016.

[15] M. Kohl, R. F. Capellmann, M. Laurati, S. U. Egelhaaf, and M. Schmiedeberg. Directed percolation identified as equilibrium pre-transition towards non-equilibrium arrested gel states. *Nat. Commun.*, 7:11817, 2016.

[16] M. Takahashi, M. Kobayashi, and K. A. Takeuchi. Universal critical behavior at a phase transition to quantum turbulence. *arXiv preprint arXiv:1609.01561*, 2016.

[17] R. Löw, H. Weimer, U. Krohn, R. Heidemann, V. Bendkowsky, B. Butscher, H. P. Büchler, and T. Pfau. Universal scaling in a strongly interacting Rydberg gas. *Phys. Rev. A*, 80:033422, 2009.

[18] S. Helmrich, A. Arias, and S. Whitlock. Scaling of a driven atomic gas from the weakly-dressed to the quantum critical regime. *arXiv preprint arXiv:1605.08609*, 2016.

[19] H. Schempp, G. Günter, M. Robert-de Saint-Vincent,

C. S. Hofmann, D. Breyel, A. Komnik, D. W. Schönleber, M. Gärttner, J. Evers, S. Whitlock, and M. Weidemüller. Full counting statistics of laser excited Rydberg aggregates in a one-dimensional geometry. *Phys. Rev. Lett.*, 112:013002, 2014.

[20] N. Malossi, M. M. Valado, S. Scotto, P. Huillery, P. Pillet, D. Ciampini, E. Arimondo, and O. Morsch. Full counting statistics and phase diagram of a dissipative Rydberg gas. *Phys. Rev. Lett.*, 113:023006, 2014.

[21] A. Urvoy, F. Ripka, I. Lesanovsky, D. Booth, J. P. Shaffer, T. Pfau, and R. Löw. Strongly correlated growth of Rydberg aggregates in a vapor cell. *Phys. Rev. Lett.*, 114:203002, 2015.

[22] M. M. Valado, C. Simonelli, M. D. Hoogerland, I. Lesanovsky, J. P. Garrahan, E. Arimondo, D. Ciampini, and O. Morsch. Experimental observation of controllable kinetic constraints in a cold atomic gas. *Phys. Rev. A*, 93:040701, 2016.

[23] C. Simonelli, M. M. Valado, G. Masella, L. Asteria, E. Arimondo, D. Ciampini, and O. Morsch. Seeded excitation avalanches in off-resonantly driven Rydberg gases. *Journal of Physics B: Atomic, Molecular and Optical Physics*, 49(15):154002, 2016.

[24] F. Letscher, O. Thomas, M. Fleischhauer T. Niederprüm, and H. Ott. Bistability vs. metastability in driven dissipative Rydberg gases. *arXiv preprint arXiv:1611.00627*, 2016.

[25] C. Carr, R. Ritter, C. G. Wade, C. S. Adams, and K. J. Weatherill. Nonequilibrium phase transition in a dilute Rydberg ensemble. *Phys. Rev. Lett.*, 111:113901, 2013.

[26] N. Šibalić, C. G. Wade, C. S. Adams, K. J. Weatherill, and T. Pohl. Driven-dissipative many-body systems with mixed power-law interactions: Bistabilities and temperature-driven nonequilibrium phase transitions. *Phys. Rev. A*, 94:011401, 2016.

[27] C. Ates, T. Pohl, T. Pattard, and J. M. Rost. Antiblockade in Rydberg excitation of an ultracold lattice gas. *Phys. Rev. Lett.*, 98:023002, 2007.

[28] T. Amthor, C. Giese, C. S. Hofmann, and M. Weidemüller. Evidence of antiblockade in an ultracold Rydberg gas. *Phys. Rev. Lett.*, 104:013001, 2010.

[29] I. Lesanovsky and J. P. Garrahan. Kinetic constraints, hierarchical relaxation, and onset of glassiness in strongly interacting and dissipative Rydberg gases. *Phys. Rev. Lett.*, 111(21):215305, 2013.

[30] I. Lesanovsky and J. P. Garrahan. Out-of-equilibrium structures in strongly interacting Rydberg gases with dissipation. *Phys. Rev. A*, 90(1):011603, 2014.

[31] T. Amthor, M. Reetz-Lamour, S. Westermann, J. Denskat, and M. Weidemüller. Mechanical effect of van der Waals interactions observed in real time in an ultracold Rydberg gas. *Phys. Rev. Lett.*, 98:023004, 2007.

[32] D. Comparat and P. Pillet. Dipole blockade in a cold Rydberg atomic sample. *J. Opt. Soc. Am. B*, 27(6):A208–A232, 2010.

[33] R. Löw, H. Weimer, J. Nipper, J. B. Balewski, B. Butscher, H. P. Büchler, and T. Pfau. An experimental and theoretical guide to strongly interacting Rydberg gases. *J. Phys. B*, 45(11):113001, 2012.

[34] N. Thaicharoen, A. Schwarzkopf, and G. Raithel. Measurement of the van der Waals interaction by atom trajectory imaging. *Phys. Rev. A*, 92:040701, 2015.

[35] R. Celistrino Teixeira, C. Hermann-Avigliano, T. L. Nguyen, T. Cantat-Moltrecht, J. M. Raimond, S. Haroche, S. Gleyzes, and M. Brune. Microwaves probe dipole blockade and van der Waals forces in a cold Rydberg gas. *Phys. Rev. Lett.*, 115:013001, 2015.

[36] R. Faoro, C. Simonelli, M. Archimi, G. Masella, M. M. Valado, E. Arimondo, R. Mannella, D. Ciampini, and O. Morsch. van der Waals explosion of cold Rydberg clusters. *Phys. Rev. A*, 93:030701, 2016.

[37] T. G. Walker and M. Saffman. Consequences of Zeeman degeneracy for the van der Waals blockade between Rydberg atoms. *Phys. Rev. A*, 77:032723, 2008.

[38] C. Ates, T. Pohl, T. Pattard, and J. M. Rost. Many-body theory of excitation dynamics in an ultracold Rydberg gas. *Phys. Rev. A*, 76:013413, 2007.

[39] D. Petrosyan, M. Höning, and M. Fleischhauer. Spatial correlations of Rydberg excitations in optically driven atomic ensembles. *Phys. Rev. A*, 87:053414, 2013.

[40] Z. Cai and T. Barthel. Algebraic versus exponential decoherence in dissipative many-particle systems. *Phys. Rev. Lett.*, 111:150403, 2013.

[41] M. Marcuzzi, J. Schick, B. Olmos, and I. Lesanovsky. Effective dynamics of strongly dissipative Rydberg gases. *J. Phys. A: Math. Theor.*, 47(48):482001, 2014.

[42] See the Supplemental Material for details.

[43] M. Marcuzzi, E. Levi, W. Li, J. P. Garrahan, B. Olmos, and I. Lesanovsky. Non-equilibrium universality in the dynamics of dissipative cold atomic gases. *New J. Phys.*, 17(7):072003, 2015.

[44] H. K. Janssen. Renormalized field theory of the Gribov process with quenched disorder. *Phys. Rev. E*, 55:6253–6256, 1997.

[45] R. Cafiero, A. Gabrielli, and M. A. Muñoz. Disordered one-dimensional contact process. *Phys. Rev. E*, 57:5060–5068, 1998.

[46] A. G. Moreira and R. Dickman. Critical dynamics of the contact process with quenched disorder. *Phys. Rev. E*, 54:R3090–R3093, 1996.